Crosstalk-Aware Core and Spectrum Assignment in a Multicore Optical Link With Flexible Grid

Cristina Rottondi, Paolo Martelli, Pierpaolo Boffi, Luca Barletta, and Massimo Tornatore

***Abstract*— Multicore fibers (MCFs) are one of the main technological enablers for space-division multiplexing. In principle, MCFs could scale the fiber capacity by a factor equal to the number of cores, but in practice such increase is hindered by transmission impairments due to the inter-core crosstalk between adjacent lit cores. The entity of such crosstalk depends on the number of cores and on their disposition within the fiber cladding, and also on the baud rate and modulation format used for transmission. As first MCF applications are expected over point-to-point systems, in this paper we concentrate on the resource allocation over a single link. Specifically, we study the Baud rate, Modulation format, Core and Spectrum Assignment problem in a multicore flexi-grid link, considering distance-adaptive reaches for different baud rates, modulation formats, and crosstalk impairments. We show that the problem is NP-hard and provide two integer linear programs, as well as heuristic approaches to solve it over large/practical traffic instances. Our problem formulations incorporate modeling of the exact inter-core crosstalk contributions depending on the number of lit neighbor cores. Numerical results are provided in a high-spatial-efficiency 19-core fiber considering different transmission impairment conditions.**

***Index Terms*— Multi-core optical fibers, core and spectrum assignment, inter-core crosstalk.**

I. Introduction

Space Division Multiplexing (SDM) techniques are under investigation as means to increase the capacity of optical networks. Multi-core fibers (MCFs), constituted by a group of physically-separated single-mode cores within the same cladding, have been recently demonstrated [1], [2] and several MCF network architectures are being proposed [3]–[5]. Theoretically, MCF can scale fiber capacity by a factor equal to the number of cores, while increasing core density with respect to the use of bundles of separate fibers. However, inter-core crosstalk between adjacent cores introduces transmission impairments, leading to a tradeoff between increase in utilization of the cores and decrease in signal reach. The entity of such crosstalk depends on the number of cores in the same fiber, on their refraction index profile and disposition within the cladding, and on the diameter of the fiber itself [2].

First demonstrations of MCF transmission have mostly focused on point-to-point single-link transmission (see recent experiments of beyond Pbps transmission in [6]). A recent multicore testbed demonstrated in [7] considers a network composed by 3 links, only two out of those supporting multicore transmission. As a matter of fact, practical adoption of MCF in optical networks requires the development of network devices such as optical amplifiers and optical switches capable of supporting multicore transmission, but the research and prototyping of such devices is currently still in its infancy (see [8] for a preliminary assessment of a spatial light modulator optical switch for MCF). Most probably, also first operational implementations of MCF transmission will appear on point-to-point systems: for example, application of MCF for intra-datacenter high-speed transmission has been devised [9]. However, even in this simplified scenario, optimal resource allocation is not trivial, due to the contrasting factors discussed before.

Hence, in this paper we consider a single multi-core flexi-grid optical link and we focus on the problem of how to identify the core, spectrum, baud rate and modulation format assignments that optimize a given objective, e.g. spectrum occupation or number of transceivers to serve a given traffic. More formally, given a set of traffic requests to be transmitted over a multicore link, the problem consists in i) assigning a core to every traffic flow; ii) choosing a combination of baud rate and modulation format for the transceivers serving each traffic flow; iii) allocating an optical channel for each traffic flow, large enough to accommodate the required transceivers, ensuring spectral contiguity of its spectrum slots and separation of spectrally-adjacent channels by means of guardbands over each core. Note that using multiple modulation formats and baud rates leads to a trade-off between transmission reaches, maximum tolerated inter-core crosstalk and transmission capacity: low baud rates and modulation formats with low spectral efficiency achieve longer reaches and tolerate higher crosstalk, but increase spectrum and transceiver usage. Conversely, high baud rates and modulation formats with high spectral efficiency reduce the number of transceivers (and thus specrum usage) needed to serve a traffic demand, at the price of lower reaches and low inter-core crosstalk tolerance, which imposes to leave unoccupied some spectrum portions

Manuscript received April 10, 2018; revised September 3, 2018 and November 9, 2018; accepted November 12, 2018. Date of publication November 16, 2018; date of current version March 15, 2019. This work is partially funded by the European Union's Horizon 2020 research and innovation programme under grant agreement PASSION No 780326. M. Tornatore acknowledges support from NSF grant 1716945. The associate editor coordinating the review of this paper and approving it for publication was M. Secondini. *(Corresponding author: Cristina Rottondi.)*

C. Rottondi is with the Dalle Molle Institute for Artificial Intelligence, University of Lugano, 6900 Lugano, Switzerland, and also with the University of Applied Sciences and Arts of Southern Switzerland, 6928 Manno, Switzerland (e-mail: cristina.rottondi@supsi.ch).

P. Martelli, P. Boffi, L. Barletta, and M. Tornatore are with the Dipartimento di Elettronica, Informazione e Bioingegneria, Politecnico di Milano, 20133 Milan, Italy (e-mail: pierpaolo.boffi@polimi.it; paolo.martelli@polimi.it; luca.barletta@polimi.it; massimo.tornatore@polimi.it).

Color versions of one or more of the figures in this paper are available online at http://ieeexplore.ieee.org.

Digital Object Identifier 10.1109/TCOMM.2018.2881697

of the neighbor cores. Moreover, as the channel bandwidth needed to serve a demand depends on the transceiver capacity, which is a function of the baud rate and modulation format adopted for transmission, the usage of multiple baud rates and modulation formats makes it impossible to pre-compute the bandwidth requirement of a traffic request and to use it as problem input, therefore the channel bandwidth becomes an optimization variable of the problem. It follows that the problem complexity is increased with respect to a scenario where a single combination of baud rate and modulation format is available.

We define this problem as Baud rate, Modulation format, Spectrum and Core Assignment (BMSCA) and show that it is NP-hard. Moreover, we provide two alternative Integer Linear Programs (ILPs), as well as heuristic algorithms to solve large problem instances. Though some studies on static and dynamic approaches for spectrum and core assignment in MCFs have already appeared [10], to the best of our knowledge, this is the first attempt to model and solve it for a given offered traffic in presence of multiple modulation formats and by taking into account the crosstalk impact depending on the number of adjacent interfering cores on the link power budget. Our numerical results provide useful insights on the structure of the optimal solutions and show that the proposed heuristic algorithms closely approaches the optimum in most of the considered scenarios.

The remainder of the paper is organized as follows: Section II briefly overviews the related scientific literature, whereas in Section III we describe the network and transceiver model and we discuss how to compute the transmission reaches over MCFs for different baud rates and modulation formats. The mathematical formulations used to optimally solve the BMSCA problem with MCFs are presented in Section IV, whereas heuristic approaches are discussed in Section V. Numerical results are commented in Section VI. Finally, Section VII concludes the paper.

II. Related Work

Some networking problems in MCF networks have been already investigated in recent studies (see survey [11] for a thorough overview). Reference [12] was the first study to deal with resource allocation in a MCF network. The authors proposed an ILP and a heuristic algorithm for Routing, Spectrum and Core Allocation (RSCA) in flexi-grid MCF networks, considering intercore crosstalk and minimizing the index of the rightmost occupied spectrum slice over the whole network. Even though in in our paper we consider similar optimization objectives, [12] assumes the adoption of a single modulation format. A variation of the model is proposed in [13] to minimize the overall network cost due to switching modules required for the different cores of the input/output fibers in optical crossconnects.

An ILP and a heuristic algorithm for the anycast planning problem in flexi-grid MCF networks are discussed in [14], assuming that a single modulation format is adopted for transmission. All the studies mentioned so far adopt a worst-case approach for crosstalk calculation, which consists in considering all the neighbor cores as interfering, regardless to their actual spectrum occupation.

In [15], an ILP investigating the impact of MIMO-based crosstalk suppression on the RSCA problem is proposed. With the MIMO technology, several co-propagating signals over the same wavelengths of adjacent cores can be recovered if they are all received and processed at the same receiving node, because the accumulated inter-core crosstalk can be eliminated via digital signal processing at their common receiver. The authors evaluate the benefits of MIMO-enabled crosstalk suppression w.r.t. a benchmark scenario where MIMO technology is not adopted. The formulation incorporates an additive crosstalk model, i.e., every traffic request is assumed to suffer an amount of crosstalk proportional to the number of neighboring cores, and the total crosstalk amount must not exceed a given threshold. A similar crosstalk model is used in [16], where an ILP minimizing the total capital expenditures for the deployment of an optical network with both single-core and multi-core links is provided. In our model, we adopt the same crosstalk modeling approach but we do not make use of MIMO receivers. Conversely, we consider a flexi-grid scenario with multiple baud rates and modulation formats, whereas in [15] and [16] a standard WDM grid and pre-defined bandwidth demands for each traffic requests are considered.

In [17], a low-complexity node-arc-based ILP formulation for RSCA with crosstalk worst-case approach is proposed and compared to a reference formulation which models crosstalk exactly and allows for definition of different crosstalk thresholds. A crosstalk-aware heuristic algorithm is also proposed. Also in this study, pre-defined bandwidth demands for each traffic requests are assumed. Note that when considering multiple transceiver modulation formats and baud rates, the complexity of the problem is increased, as the channel bandwidth cannot be precomputed and becomes an optimization variable: indeed, depending on the number of adjacent lit cores and on the link length, some combinations of baud rates and modulation formats will be infeasible and some others will result feasible but, given the spectral efficiency of the considered modulation format and the considered baud rate, each of them will require a different channel width to accommodate the traffic.

In [10] and [18], a heuristic for RSCA with a static traffic matrix is proposed; reach values of different modulations formats are calculated considering that SNR degradation is mainly induced by ASE noise and crosstalk. In our paper we refine this reach calculation by considering the actual number of lit neighboring cores when evaluating the crosstalk and by also taking into account the reach limitations due to nonlinear effects. Moreover, we compute reach values for MCF transmission considering not only multiple modulation formats but also different transceiver baud rates.

Under assumption of dynamic traffic, [4], [19], and [20] discuss several heuristic algorithms for spectrum and core allocation in an on-demand scenario for joint reduction of intercore crosstalk and spectrum fragmentation. Reference [21] extends [19] in the framework of the novel Architecture-on-Demand concept. The proposed methods are based on core/spectrum prioritization and classification criteria, which

privilege the assignment of traffic requests to non-adjacent cores or to non-overlapping spectrum portions in adjacent cores. Reference [22] further extends the framework, considering multiple modulation formats, but the choice of the format to be used to serve each traffic request is pre-determined before performing core and spectrum assignment, based on the number of hops traversed by the lightpath depending on its route, which is determined during an initial routing phase. Reference [23] proposes five heuristics for dynamic RSCA, but does not take into account crosstalk impairments. A heuristic algorithm for dynamic RSCA in presence of MIMO Digital Signal Processing compensation techniques is proposed in [24], whereas a heuristic for RSCA re-optimization in a software defined network framework is discussed in [25]. In [26] and [27], heuristic algorithms for dynamic RSCA over trench-assisted MCFs (i.e., fibers with index trench structure around each core, which achieve drastic crosstalk reduction w.r.t. standard fibers with step index) are discussed. Our heuristic approach focuses on a static traffic scenario and on a single MCF optical link, and accounts for multiple modulation formats and a detailed crosstalk modeling that allows for investigation of the most effective tradeoff between spectral efficiency and number of lit cores.[1]

III. Flexi Grid and Reach Model in Presence of Crosstalk

A. Reach Model

We consider transmission of polarization-multiplexed (PM) optical signals in a high-spatial-efficient 19-core fiber [29]. Compared to other commonly-considered 7-core and 12-core fibers [2], the 19-core fiber ensures higher capacity and reaches a spatial efficiency of 7.4.[2]

We assess the maximum transmission reach for several modulation formats, to guarantee a target Bit Error Rate (BER) of $3.8 \cdot 10^{-3}$ at 7%-overhead FEC threshold level. We assume that the spectrum is divided in slices of 12.5 GHz and that transceivers support polarization-multiplexed (PM) QPSK and M-QAM modulated signals, with $M = 4, 8, 16, 32, 64$, at a baud rate $B = 28, 14$ GBaud, occupying an optical bandwidth F of 37.5 and 25 GHz, respectively. Neighbor channels must be separated by a guardband of given spectral width G. Moreover, we consider a WDM balanced multi-span optically-amplified link, where multicore EDFAs [30] with noise figure of 6 dB are used to exactly compensate for the losses of each span of length 50 km. The chosen span length is shorter than a typical terrestrial span length for single-mode fiber links ($80 - 100$ km), due to the fact that multicore EDFA amplifiers [30], [31] show a smaller gain with respect to single-mode EDFA amplifiers, especially in case of high number of cores. Therefore, we envisage that 50 km could be a realistic span length in future multicore fiber links with 19-core EDFA. The 19-core MCF considered in our paper is characterized by an attenuation coefficient of 0.227 dB/km [29], resulting in a 50-km span attenuation of 11.4 dB. In addition to the optical noise introduced by EDFAs, we also take into account the signal impairments due to the nonlinear optical effects (evaluated by using the Gaussian noise model in [32]) and the inter-core crosstalk (evaluated as an equivalent Gaussian noise [33]). To account for the non-ideal behavior of the coherent receiver and for a filtering penalty, optical margins of 2 and 1.5 dB are introduced at B equal to 28 and 14 Gbaud, respectively. We determined the optimal values of the total transmitted power (over all wavelengths and polarizations) to maximize the reach, obtaining 18.5 and 18.8 dBm, at B equal to 28 and 14 Gbaud, respectively. Two different crosstalk scenarios are considered: i) average crosstalk of -25 dB between two adjacent cores after a single span propagation (as inferred from measurements reported in [29]); ii) average crosstalk of -40 dB, to envisage possible future crosstalk reduction in next years. In both scenarios we consider two different total spectrum widths, namely 4 THz and 0.5 THz. The former considers a fully occupied C-band, whereas the latter considers a lowly-loaded link. Moreover, we assume the crosstalk coming from non-adjacent cores as negligible and report the total crosstalk per span due to interference of adjacent lit cores. Note that we do not consider MIMO processing at the receiver, i.e., we treat interference as noise. This assumption is conservative since it does not exploit the benefit of MIMO DSP at the receiver.

Tables I and II report the transmission reaches calculated for each combination of baud rate, modulation format and number of adjacent lit cores, γ, following the assumptions commented above. The total average crosstalk experienced by a given core is the sum of the individual average crosstalk contributions from each neighbor (i.e., total crosstalk depends on the total number of neighboring lit cores). In the considered 19-core MCF, where the cores are disposed in a hexagonal close-packed arrangement, the number of lit neighboring cores varies from a minimum of 0 (i.e., no inter-core crosstalk) to a maximum of 6.

From the two Tables, it is evident that a reduction of the reach is due to the crosstalk originated by the neighboring cores, especially in the scenario of an average single-span crosstalk of -25 dB between two adjacent cores, with respect to the case of no crosstalk. The reported reaches are all calculated by taking into account the fiber-optic Kerr nonlinear effect through the GN model, using the formula of [32, eq. (15)], which accounts for the effective bandwidth occupation of each wavelength channel (that is 28 GHz and 14 GHz, respectively). Moreover, to quantify the role of fiber nonlinearity, we also evaluated the reaches in absence of both nonlinearity and crosstalk. In the case of a symbol rate of 28 GBd, the calculated reaches are 8100, 3250, 1750, 900 and 400 km for 4-, 8-, 16-, 32- and 64-QAM modulation formats, respectively. Comparing these values with the reaches of Table I calculated taking into account the Kerr nonlinear

[1] Note that a preliminary version of this study appeared in [28]. With respect to [28], this paper provides extensive reach computations over a 19-core fiber link for different combinations of baud rates and modulation formats, reports the details of two Integer Linear Programs to optimally solve the BMSCA problem, and introduces two novel heuristic approaches to tackle large instances.

[2] Spatial efficiency is calculated as the number of cores by the ratio between the cladding cross-section areas of the considered MCF and a corresponding single mode fiber, by compacting 19 cores in a cladding diameter of $200\mu m$.

TABLE I

REACH VALUES (km) FOR VARIOUS MODULATION FORMATS AT 28 GBAUD AND INCREASING NUMBER OF NEIGHBORING LIT CORES FOR A 19-CORE FIBER, ASSUMING A CROSSTALK CONTRIBUTION OF EITHER −25 dB (TOP ROWS) OR −40 dB (BOTTOM ROWS) PER SPAN BY EACH NEIGHBOR

Lit neighbor cores (γ)	Crosstalk per span (dB)	Calculated reach (km) for 4-THz spectrum width					Calculated reach (km) for 0.5-THz spectrum width				
		QPSK	8-QAM	16-QAM	32-QAM	64-QAM	QPSK	8-QAM	16-QAM	32-QAM	64-QAM
0	none	5200	2050	1100	550	250	6050	2400	1300	650	300
1	-25.0	1100	400	200	100	50	1100	450	200	100	50
2	-22.0	600	200	100	50	0	600	250	100	50	0
3	-20.2	400	150	50	0	0	400	150	50	0	0
4	-19.0	300	100	50	0	0	300	100	50	0	0
5	-18.0	250	100	50	0	0	250	100	50	0	0
6	-17.2	200	50	0	0	0	200	50	0	0	0
0	none	5200	2050	1100	550	250	6050	2400	1300	650	300
1	-40.0	4650	1850	1000	500	250	5300	2100	1150	550	250
2	-37.0	4200	1650	900	450	200	4750	1900	1000	500	250
3	-35.2	3850	1500	800	400	200	4300	1700	900	450	200
4	-34.0	3550	1400	750	400	150	3900	1550	800	400	200
5	-33.0	3300	1300	700	350	150	3600	1400	750	400	150
6	-32.2	3050	1200	650	300	150	3300	1300	700	350	150

TABLE II

REACH VALUES (km) FOR VARIOUS MODULATION FORMATS AT 14 GBAUD AND INCREASING NUMBER OF NEIGHBORING LIT CORES FOR A 19-CORE FIBER, ASSUMING A CROSSTALK CONTRIBUTION OF EITHER −25 dB (TOP ROWS) OR −40 dB (BOTTOM ROWS) PER SPAN BY EACH NEIGHBOR

Lit neighbor cores (γ)	Crosstalk per span (dB)	Calculated reach (km) for 4-THz spectrum width					Calculated reach (km) for 0.5-THz spectrum width				
		QPSK	8-QAM	16-QAM	32-QAM	64-QAM	QPSK	8-QAM	16-QAM	32-QAM	64-QAM
0	none	9050	3600	1950	1000	500	10450	4150	2250	1150	550
1	-25.0	1350	500	250	150	50	1350	500	250	150	50
2	-22.0	700	250	150	50	0	700	250	150	50	0
3	-20.2	450	200	100	50	0	450	200	100	50	0
4	-19.0	350	150	50	0	0	350	150	50	0	0
5	-18.0	300	100	50	0	0	300	100	50	0	0
6	-17.2	250	100	50	0	0	250	100	50	0	0
0	none	9050	3600	1950	1000	500	10450	4150	2250	1150	550
1	-40.0	7650	3050	1650	850	400	8600	3450	1850	950	450
2	-37.0	6650	2650	1400	700	350	7350	2900	1550	800	400
3	-35.2	5850	2350	1250	650	300	6400	2550	1350	700	350
4	-34.0	5250	2100	1100	550	250	5650	2250	1200	600	300
5	-33.0	4750	1500	1000	500	250	5050	2000	1050	550	250
6	-32.2	4350	1700	900	450	200	4600	1800	950	500	250

effect in case of wavelength channels over the whole C-band (i.e., 4-THz spectrum width) and without crosstalk, we see that the nonlinear penalty leads to a reach reduction between 35% and 40%. In the case of a 14 GBaud symbol rate, the calculated reaches are 12900, 5150, 2750, 1450 and 700 km for 4-, 8-, 16-, 32- and 64-QAM modulation formats, respectively. Comparing these values with the reaches of Table II calculated in the condition of 4-THz spectrum width and no crosstalk, we see that the nonlinear penalty leads to a reach reduction of about 30%.

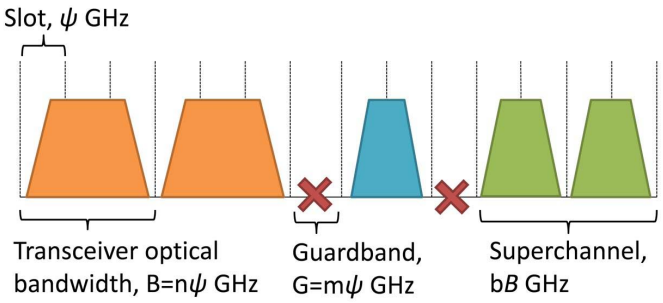

Fig. 1. The optical flexi-grid.

B. Flexi Grid Model

As depicted in Fig. 1, we assume that the optical spectrum is subdivided in a flexi-grid of frequency slots of granularity ψ GHz. The available spectrum portion on every core is $S = k\psi$ GHz (with k integer).

If a traffic request exceeds the capacity of a single transceiver, it can be served by a number b of adjacent transceivers forming a *superchannel*, which is handled and switched as a single entity [34], given that it is separated from the adjacent (super)channels by a guardband of $G = m\psi$ GHz (with m integer), in order to avoid overlapping and crosstalk among neighbor signals (in Fig. 1, a 1 slot guardband is assumed). The superchannel bandwidth can be computed as bB, where $B = n\psi$ is the transceiver optical bandwidth, expressed as integer multiple of the slot width.

Transceivers working at baud rates $B = 14$ GBd (respectively $B = 25$ GBd) occupy $2\phi = 25$ GHz (respectively $3\phi = 37$ GHz). In the remainder of this paper, we will adopt the transmission reaches reported in Tables I and II.

IV. The BMSCA Problem With MCF

In this Section we first formally define the BMSCA problem, then provide two alternative ILP formulations to optimally solve it, compare their respective complexities and prove the NP-hardness of the problem.

A. Problem Definition and Assumptions

Given a multicore link of fixed length, the adjacency matrix of its cores (which depends on their physical placement within the fiber cladding) and a number of traffic requests of arbitrary volumes, the BMSCA problem consists in:

- attributing a core used for transmission to every lightpath.
- choosing the number of transceivers serving the traffic streamed over each lightpath, as well as the combination of baud rate and modulation format adopted for transmission.
- allocating a (super)channel for each lightpath (with bandwidth large enough to accommodate the transceiver pair(s) necessary to serve the traffic flow), ensuring spectral contiguity between spectrum slots associated to the same lightpath and separation of spectrally adjacent (super)channels by means of guardbands.

The core and spectrum assignment and the choice of transceivers' baud rates and modulation formats is subject to crosstalk constraints: more in detail, the reach of a given combination of baud rate and modulation format used to serve a traffic request over a lightpath allocated on a core depends on the total amount of inter-core crosstalk, which in turn depends on the number of adjacent lit cores where the same spectrum portion is occupied for transmission by other lightpaths.

B. Slice-Based Formulation

Sets:

- C: set of cores $1 \dots |C|$
- M: set of modulation formats $1 \dots |M|$
- B: set of baud rates $1 \dots |B|$
- S: set of spectrum slices $1 \dots |S|$
- T: set of traffic requests $1 \dots |T|$

Parameters:

- F_b: optical bandwidth (number of slices) of a transceiver operating at baud rate $b \in B$
- R_{mb}: capacity of a transceiver operating at baud rate $b \in B$ and modulation format $m \in M$ (Gbps)
- G: guardband width (number of slices)
- ν_t: volume of traffic request $t \in T$ (Gbps)
- $\Gamma_{cc'}$: binary parameter set to 1 if cores $c \in C$ and $c' \in C$: $c \neq c'$ are adjacent
- n_{mbc}: binary parameter set to 1 if the reach of a transceiver operating at modulation format $m \in M$ and baud rate $b \in B$ in presence of $c-1$ adjacent lit cores is greater than the link length L
- Q: big constant, greater than $|S|$ and $|C|$

Variables:

- y_{tc}: binary variable, it is 1 if traffic request $t \in T$ is allocated over core $c \in C$
- z_{tsc}: binary variable, it is 1 if traffic request $t \in T$ occupies slice $s \in S$ of core $c \in C$
- f_{ts}: binary variable, it is 1 if $s \in S$ is the rightmost slice of the optical (super)channel used to serve request $t \in T$
- w_{tmb}: integer positive variable indicating the number of transceivers operating at baud rate $b \in B$ and modulation format $m \in M$ used to serve request $t \in T$
- β_{tmb}: binary variable, it is 1 if transceivers operating at baud rate $b \in B$ and modulation format $m \in M$ are used to serve request $t \in T$
- x_{tc}: binary variable, it is 1 if the (super)channel of request t suffers of interference due to occupation of at most $c-1$ adjacent cores (on at least one of the corresponding (super)channel slices)
- ϕ: integer positive variable indicating the index of the rightmost occupied slice over all cores

Objective Function:

$$\alpha_1 \sum_{t \in T, m \in M, b \in B} 2w_{tmb} + \alpha_2 \phi \tag{1}$$

By properly tuning the value of the two multiplicative factors α_1, α_2, we minimize either the index of the rightmost occupied spectrum slice H_s (when $\alpha_1 \ll \alpha_2$) or the number of installed transceivers N_t (when $\alpha_1 \gg \alpha_2$). Note that, in case of multiple configurations providing minimum H_s (resp. N_t), this

objective functions allows to choose the one which minimizes N_t (resp. H_s).

Constraints:

$$\sum_{c\in C} y_{tc} = 1 \quad \forall t \in T \tag{2}$$

$$\sum_{m\in M, b\in B} w_{tmb} R_{mb} \geq \nu_t \quad \forall t \in T \tag{3}$$

$$\sum_{m\in M, b\in B} \beta_{tmb} = 1 \quad \forall t \in T \tag{4}$$

$$w_{tmb} \leq Q\beta_{tmb} \quad \forall t \in T, m \in M, b \in B \tag{5}$$

$$\sum_{s\in S, c\in C} z_{tsc} = \sum_{m\in M, b\in B} w_{tmb} F_b + G \quad \forall t \in T \tag{6}$$

$$z_{tsc} + f_{ts} \geq z_{t(s-1)c} \quad \forall t \in T, c \in C, s \in S\colon s > 1 \tag{7}$$

$$\sum_{c\in C} z_{tsc} s \leq \sum_{s\in S} f_{ts} s \quad \forall t \in T, s \in S \tag{8}$$

$$\sum_{s\in S} f_{ts} = 1 \quad \forall t \in T \tag{9}$$

$$f_{ts} \leq \phi \quad \forall t \in T, s \in S \tag{10}$$

$$Q y_{tc} \geq \sum_{s\in S} z_{tsc} \quad \forall t \in T, c \in C \tag{11}$$

$$\sum_{t\in T} z_{tsc} \leq 1 \quad \forall s \in S, c \in C \tag{12}$$

$$\sum_{c\in C} (c-1) x_{tc} + Q(1 - z_{tsc}) \geq \sum_{c'\in C, t'\in T: t'\neq t \wedge c'\neq c} z_{t'sc'} \Gamma_{cc'} \quad \forall t \in T, s \in S, c \in C \tag{13}$$

$$\sum_{c\in C} x_{tc} = 1 \quad \forall t \in T \tag{14}$$

$$\beta_{tmb} + x_{tc} - 1 \leq n_{mbc} \quad \forall t \in T, m \in M, b \in B, c \in C \tag{15}$$

Constraint 2 imposes that each traffic request is allocated in exactly one core, whereas Constraint 3 ensures that the total capacity of the transceivers used to serve a request is sufficient to accommodate its traffic volume. Constraints 4 and 5 impose that multiple baud rates/modulation formats do not coexist in a single (super)channel.[3] Constraint 6 guarantees that the number of slices allocated to a request equals the optical bandwidth of the (super)channel formed by contiguously placing the transceivers required to serve it. Constraint 7 imposes contiguity among the slices allocated to each request, whereas Constraint 8 sets the variable f_{ts} to the rightmost slice number used to serve request t (note that, since the variables z_{tsc} and f_{ts} are binary, the index s is used as multiplicative factor to obtain the corresponding slice number). Constraint 9 guarantees that only one ending slice is selected for each traffic request and Constraint 10 sets variable ϕ to the rightmost occupied slice over all cores. Constraint 11 ensures coherence between the values of the variables y_{tc} and z_{tsc}, whereas Constraint 12 ensures that each slice of every core is occupied by at most one traffic request. Constraints 13 and 14 count, for each (super)channel allocated on a given core, the number of neighbor cores where at least one of the corresponding slices is occupied. Finally, Constraint 15 guarantees that only one of the feasible choices of baud rates and modulation formats is used for the transceivers serving each traffic request, i.e., the corresponding reach must exceed the link length despite the interference due to the occupation of (part of) the same (super)channel spectrum portion in the neighboring cores. More in detail, for each slice included in the (super)channel that serves a request, the number of neighboring cores where the same slice is occupied is counted. The maximum number of neighbors is then considered (e.g., if a channel occupies three slices, the first slice is occupied in one of the neighbor cores, the second slice is occupied in three neighbor cores and the third one is occupied in two neighbor cores, then the number of neighbors considered for the computation of the reach limitations is three).

[3]Such constraints could be omitted if coexistence of multiple transceiver configurations in a superchannel is allowed.

C. Configuration-Based Formulation

An alternative ILP formulation for the BMSCA problem considers the spectrum slices one at a time and enumerates the configurations of cores in which such slice is in use. Therefore, in addition to the previous sets, the set K including all the possible configurations of lit cores is introduced, as well as a boolean parameter ψ_{ck}, which is set to 1 if core $c \in C$ is lit in configuration $k \in K$. Some examples of configurations are reported in Fig. 2, where grey circles represent lit cores. Moreover, parameter n_{mbc} is replaced by n_{mbck}, which is set to 1 if the reach of a transceiver operating at baud rate $b \in B$ and modulation format $m \in M$ over core $c \in C$ is compatible with the link length when configuration $k \in K$ is adopted for a given slice. An additional binary variable η_{ks} is used to indicate if configuration $k \in K$ is used over the s-th slice of the cores, whereas variable x_{tc} is eliminated. Constraints 2-11 remain unvaried, whereas Constraints 12-15 are replaced by the following ones:

$$\sum_{k\in K} \eta_{ks} = 1 \quad \forall s \in S \tag{16}$$

$$\sum_{t\in T} z_{tsc} \leq \sum_{k\in K} \psi_{ck} \eta_{ks} \quad \forall c \in C, s \in S \tag{17}$$

$$\beta_{tmb} + \eta_{ks} + z_{tsc} - 2 \leq n_{mbck} \quad \forall t \in T, c \in C, m \in M, b \in B, k \in K, s \in S \tag{18}$$

Constraint 16 ensures that only one configuration of core usage is chosen for every spectrum slice; Constraint 17 guarantees coherence between the values of variables z_{tsc} and η_{ks}; Constraint 18 imposes reach limitations, depending on the core allocation of the considered request and on the number of adjacent lit cores.

D. Complexity Discussion

The complexity of the slice-based formulation in terms of number of variables and constraints is $O(|T| \cdot (|C| \cdot |S| + |M| \cdot |B|))$ and $O(|T| \cdot |C| \cdot (|M| \cdot |B| + |S|))$, respectively, whereas the complexity of the configuration-based formulation is $O(|S| \cdot |K| + |T| \cdot (|S| \cdot |C| + |M| \cdot |B|))$ and $O(|T| \cdot |S| \cdot |C| \cdot |M| \cdot |B| \cdot |K|)$. Note that, if all the possible configurations of cores are considered, then $|K| = 2^{|C|}$. However, such amount can be significantly reduced (e.g. by excluding symmetric configurations), though at the price of making the spectrum

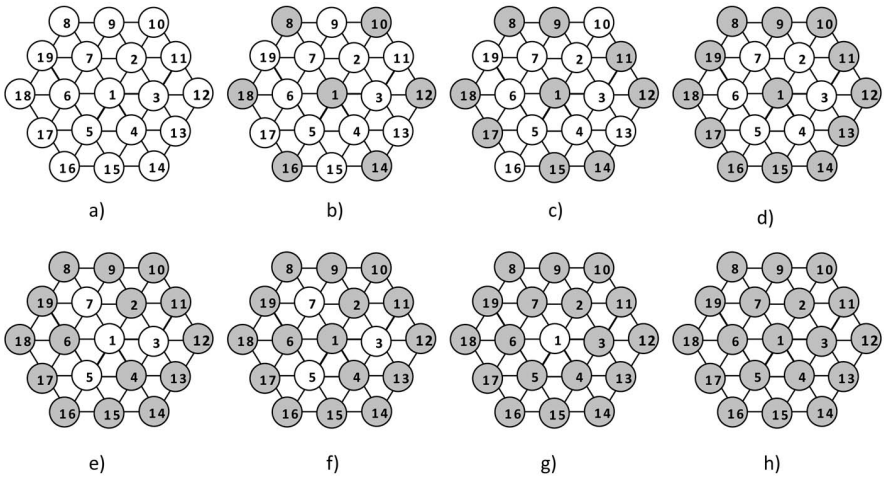

Fig. 2. The adjacency graph $\mathcal{G}$ of a 19 core fiber (a); examples of a maximal 1-independent set (b), a 2-independent set (c), a 3-independent set (d), a 4-independent set (e), a 5-independent set (f), a 6-independent set (g) and a 7-independent set (h) induced over $\mathcal{G}$.

contiguity constraint harder to be satisfied, therefore possibly forcing ϕ to higher values w.r.t. those obtained with the slice-based formulation.

Since the number of available combinations of modulation formats and baud rates can be reasonably assumed to be much lower than the number of spectrum slices, the number of variables of the slice-based formulation can be safely approximated as $O(|T|\cdot|S|\cdot|C|)$, whereas in the configuration-based formulation it can be approximated as $O(|S|(|K|+|T|\cdot|C|))$. Therefore, if $|K| \ll |T|\cdot|C|$ (which can be obtained by selecting a subset of the $2^{|C|}$ possible core configurations), the number of variables of the two formulations is comparable. Conversely, the number of constraints is always higher in the configuration-based formulation than in the slice-based formulation (i.e., approximately $O(|T|\cdot|S|\cdot|C|)$ for the slice-formulation versus $O(|T|\cdot|S|\cdot|C|\cdot|M|\cdot|B|\cdot|K|)$ for the configuration-based formulation).

Note that the configuration-based formulation, though more complex in terms of number of constraints, allows for a pre-selection of the allowed configurations of lit cores, thus helping in breaking symmetries in the problem formulation that may rise in presence of symmetric dispositions of the cores within the fiber cladding. In such case, many alternative optimal solutions can be obtained by simply renumbering some of the cores (as an example, a configuration equivalent to the one reported in Figure 2b) could be obtained by using cores 9, 11, 13, 15, 17 and 19 instead of cores 8, 10, 12, 14, 16 and 18), leading to slow convergence in the branch-and-bound algorithms implemented by ILP solvers.

We now prove the NP-hardness of the BMSCA problem.

Theorem 1: The BMCSA problem is NP-hard.

Proof: Let us consider an offered traffic with $|T| \leq |C|$ requests of equal volume ν_t. Assume that only one modulation format has a reach $r \geq L$, that such reach tolerates up to γ neighboring lit cores, and that the spectrum occupation of transceivers used to serve one traffic request is exactly $|S|$ slices (i.e., each traffic request fully occupies the available spectrum of one core). Even in this simplified case, the problem of determining a feasible traffic allocation in a MCF turns out to be equivalent to finding the *maximal ($\gamma+1$)-independent subset of vertices over a graph* $\mathcal{G}(V,E)$ [35] (where nodes $v \in V$ represent the cores and links $e(v,v') \in E$ between node pairs v, v' exist only if they represent neighboring cores), which is a well-known NP-hard problem [36].

An example of such graph $\mathcal{G}(V,E)$ for the 19-core MCF is shown in Fig. 2a). A subset of vertices $\overline{V} \subseteq V$ is defined to be $(\gamma+1)$-independent if it induces in $\mathcal{G}(V,E)$ a subgraph $\overline{\mathcal{G}}(\overline{V},\overline{E})$ (where $\overline{E} = \{e(v,v') \in E\colon v,v' \in \overline{V}\}$) of maximum degree at most γ ("degree" is the number of its outgoing links). In Fig. 2b) a 1-independent maximal set (i.e., a 1-independent set having maximum cardinality) is shown, where 7 nodes (depicted in grey) are included, each one having degree 0 (i.e., $\gamma = 0$). Figs. 2c)-2h) report other examples of $\gamma+1$-independent maximal sets, with γ ranging from 1 to 6. Under these simplified assumptions, if $|\overline{V}| \geq |T|$, allocating the $|T|$ traffic requests in the cores corresponding to the nodes of any set $\underline{V} \subseteq \overline{V}\colon |\underline{V}| = |T|$ provides a feasible solution for the BMCSA problem. In real scenarios, $|T|$ is expected to exceed $|C|$, and the volumes ν_t may assume arbitrary values. Hence, the BMCSA problem requires to solve multiple correlated $\gamma+1$-independent set problems (in the worst case, one for each slice $s \in S$). ■

V. Heuristics for the CSA Problem

As the complexity of the ILP formulations proposed in Section IV raises rapidly according to the product of the number of traffic requests, spectrum slices and number of cores, we now propose two heuristic algorithms to solve large instances of the BMCSA problem. The approaches we propose adopt a two-step procedure to solve the BMSCA problem: both first select a configuration of lit cores and then perform core and spectrum allocation of each traffic request. The procedure is repeated for different configurations and, at the end, the one providing the best solution is chosen.

A. Minimization of Spectrum Usage

Following the above described approach, let us assume we arbitrarily choose a configuration of lit cores. If the objective is spectrum usage minimization, the BMCSA problem can then be reformulated as a Parallel Machine Scheduling (PMS) problem, where cores represent processors, traffic requests represent jobs and the number of slices occupied by a request over a given core represents the time taken by a given processor to conclude the job. The spectrum occupation of a request over a given core depends on the number of adjacent lit cores which, in the analogy, represent the computational capabilities of the given processor. Note that, once the configuration of lit cores has been chosen, the number of adjacent lit cores is known and the spectrum occupation of a request to be assigned to a given core can be computed, under worst-case assumption that all the slots of the adjacent cores are occupied. The problem objective is the minimization of ϕ, i.e., the minimization of the overall time necessary to perform all the parallel jobs. Literature offers a wide range of heuristic algorithms to solve the PMS problem (see [37], [38]): in the remainder of this paper we will adopt the one proposed in [39].

Based on that, we formulate a heuristic algorithm for the BMSCA problem with spectrum usage minimization in Algorithm 1. The algorithm pre-selects a set of lit core configurations[4] (line 1), for each of them it orders the requests according to their minimum spectrum occupation - i.e. the number of spectrum slices they would require if allocated on the core allowing for the most spectrally efficient combination of baud rate and modulation format - (lines 3-10), then applies the heuristic proposed in [39] to assign requests to cores (lines 11-16). Note that [39] proposes different alternative criteria for the traffic request ordering performed at lines 7-10: in this work, we opt for the non-increasing ordering criterion based on the value of p_t computed at line 8. Finally, the configuration providing the lowest ϕ is returned (line 17). The complexity of the algorithm is $O(|K||T|\log|T|)$.

B. Minimization of the Number of Installed Transceivers

Again, let us assume we arbitrarily choose a configuration of lit cores. If the objective is the minimization of the number of installed transceivers, a possible heuristic for the BMCSA problem consists in:

1) ordering the cores based on the number of their lit neighbors, in non-decreasing order;
2) ordering traffic requests based on their volume, in non-increasing order;
3) starting from the first core of the ordered core list, assigning traffic requests from the ordered requests list with first fit approach, using the combination of modulation format and baud rate that minimizes the number of transceivers required to serve the traffic (compatibly with the link length and the number of adjacent lit cores).

[4]The number of considered core configurations can be chosen depending on the available computational time and resources. For example, considering the 19-core-fiber of this study, the set may include one maximal $\gamma+1$-independent for every γ between 0 and 6. Adding more configurations may improve the algorithm performance, at the cost of longer computational time.

Algorithm 1 Heuristic Algorithm for the BMCSA Problem With Spectrum Usage Minimization

1: on input of L, C, M, B, S, T and an arbitrary set of core configurations, K
2: **for all** configurations $k \in K$ **do**
3: **for all** lit cores c in configuration k **do**
4: considering the number of lit cores adjacent to c in configuration k, find the most spectrally efficient choice of modulation format m and baud rate b with reach exceeding the link length L
5: store the corresponding R_{mb} in a variable R^c_{mb}
6: **end for**
7: **for all** traffic request $t \in T$ **do**
8: compute $p_t = \min_{c\in k}\lceil \frac{\nu_t}{R^c_{mb}}\rceil F_b + G$
9: **end for**
10: order requests in non-increasing order of p_t in list $\mathcal{L}_T$
11: Initialize $\phi_c = 0$ on all cores $c \in k$
12: **while** $\mathcal{L}_T \neq \oslash$ **do**
13: consider the first traffic request t of list $\mathcal{L}_T$, find the core $c \in k$ such that $\phi_c + \lceil \frac{\nu_t}{R^c_{mb}}\rceil F_b + G \leq \phi_{c'} + \lceil \frac{\nu_t}{R^{c'}_{m'b'}}\rceil F_{b'} + G \ \forall c' \in k\colon c' \neq c$.
14: Assign request t to the leftmost $\lceil \frac{\nu_t}{R^c_{mb}}\rceil F_b + G$ unused slices of core c, increase ϕ_c by $\lceil \frac{\nu_t}{R^c_{mb}}\rceil F_b + G$ (if $\phi_c + \lceil \frac{\nu_t}{R^c_{mb}}\rceil F_b + G$ exceeds the total link bandwidth, set ϕ_c to ∞), eliminate t from list $\mathcal{L}_T$, store $\max_{c\in k}\phi_c$ in variable Φ_k
15: **end while**
16: **end for**
17: **return** core and spectrum assignment of configuration k with minimum Φ_k (if all configurations lead to infeasible solutions, return ∞)

The above described steps are implemented by Algorithm 2, which repeats them for different core configurations and identifies the one leading to the core and spectrum assignment with lowest amount of installed transceivers. The complexity of the algorithm is $O(|K||T|\log|T|)$.

VI. Illustrative Numerical Results

For our numerical analysis of the proposed BMCSA-solving methods, we consider a 19-core fiber link with length of 100, 500, 1000 and 1500 km and two different adjacent inter-core crosstalk values (either -25 dB or -40 dB). If not differently stated, the offered traffic consists in a variable amount (from $|T| = 1$ to 460) of traffic requests of 1 Tbps each. The optical spectrum per link is 4 THz ($|S| = 320$)[5] and guardband spacing G is 12.5 GHz. The ILP formulations of the BMSCA problem have been optimally solved using the CPLEX solver,[6] whereas the heuristic algorithms have been implemented using the MATLAB software.

[5]As conservative assumption, results have been obtained using the reach values reported in Tables I and II for a 4 THz optical spectrum width also for low traffic.

[6]Running times on a 8-core Unix machine ranged from a few minutes to a few tens of hours.

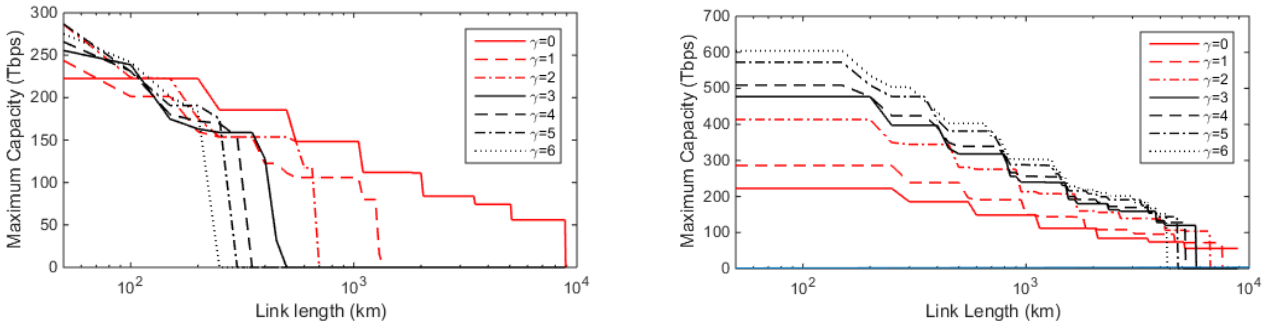

(a) -25 dB attenuation

(b) -40 dB attenuation

Fig. 3. Maximum theoretical capacity depending on the MCF link length and number of lit cores.

Algorithm 2 Heuristic Algorithm for the BMCSA Problem With Minimization of the Number of Installed Transceivers

on input of L, C, M, B, S, T and an arbitrary set of core configurations, K
for all configurations $k \in K$ **do**
  order the lit cores c in configuration k in non-decreasing order of $\sum_{c' \in k:\, c' \neq c} \Gamma_{cc'}$, store them in the ordered list $\mathcal{L}_C$.
  for all core c of list $\mathcal{L}_C$ **do**
    considering the number of lit cores adjacent to c in configuration k, find the most spectrally efficient choice of modulation format m and baud rate b with reach exceeding the link length
    store the corresponding R_{mb} in a variable R^c_{mb}
  end for
  order traffic requests in non-increasing volume order, store them in the ordered list $\mathcal{L}_T$.
  initialize variable NT_k to 0
  while $\mathcal{L}_T \neq \oslash$ **do**
    assign the first traffic request t of list $\mathcal{L}_T$ to the first core c of list $\mathcal{L}_C$ having at least $\lceil \frac{\nu_t}{R^c_{mb}} \rceil F_b + G$ free contiguous slices, with first-fit approach
    increase NT_k by $2\lceil \frac{\nu_t}{R^c_{mb}} \rceil$, eliminate t from list $\mathcal{L}_T$ (if no assignment is feasible, set NT_k to ∞)
  end while
end for
return core and spectrum assignment of configuration k with minimum NT_k (if all configurations lead to infeasible solutions, return ∞)

A. Upper Bounds on Fiber Capacity

In this subsection, we aim at answering to the following question: how many cores should be lit in a MCF to maximize capacity? Intuition suggests that the higher is the number of lit cores, the higher is the total capacity of the link. However, this proves to hold only for very short-sized links.

In order to thoroughly answer this question, we derive upper bounds on the maximum theoretical capacity (i.e., the capacity that would be obtained by transmitting over all spectrum slices without using guardbands) of a MCF. To derive this upper bound, we simply individuate the most spectrally efficient choice of baud rate b and modulation format m for a given link length and number of adjacent lit cores γ, based on the results of Tables I and II and compute the value $\lfloor \frac{|S|}{F_b} \cdot \rfloor R_{mb} \cdot W$, where W is the cardinality of the maximal $\gamma+1$-independent subset.

In Fig. 3, we plot the maximum theoretical capacity of the 19-core fiber link as a function of its length and of γ. Intuitively, using all cores (hence accepting $\gamma = 6$) is the most efficient solution for links below 100 km in the -25 dB loss per span scenario and below 5000 km in the -40 dB loss per span scenario, since highly efficient modulation formats can be used on every core even in presence of several lit neighbors (i.e., the optimal configuration is the one with 6 or 7-independent subgraphs, as depicted in Fig. 2(g-h)). Conversely, for links above 1500 km in the -25 dB loss per span scenario and above 7500 km in the -40 dB loss per span scenario, transmission can be supported only on cores with no lit neighbors (i.e., $\gamma = 0$, leading to an optimal configuration of a 1-independent subgraph, as depicted in Fig. 2(b)) using modulation formats with low spectrally efficiency (i.e., DP-8-QAM with 28 Gbd transceivers for links between 1800 and 2000 km, DP-8-QAM with 14 Gbd transceivers for links between 2000 and 3000 km, DP-QPSK with 28 Gbd transceivers for links between 3000 and 5000 km in the -25 dB loss per span scenario; DP-QPSK with 14 Gbd transceivers for links between 7500 and 8900 km in the -40 dB loss per span scenario). For links of medium length, the best tradeoff between number of lit cores and spectral efficiency of the modulation formats must be identified: e.g., in the -25 dB loss per span scenario, using less cores with higher modulation formats enables higher transmission capacity for link lengths around $400 - 1500$ km, while in the -40 dB scenario such trend emerges at much higher link lengths, i.e., above 5000 km.

It follows that the optimal choice of the number of cores to be lit depends on both the link length and on the crosstalk intensity and that the intuitive approach "the more, the better" proves not to be a general rule. This preliminary analysis motivates our following numerical assessment, that shows how our ILP- and heuristic-based optimization strategies can find the best solution to the BMCSA problem.

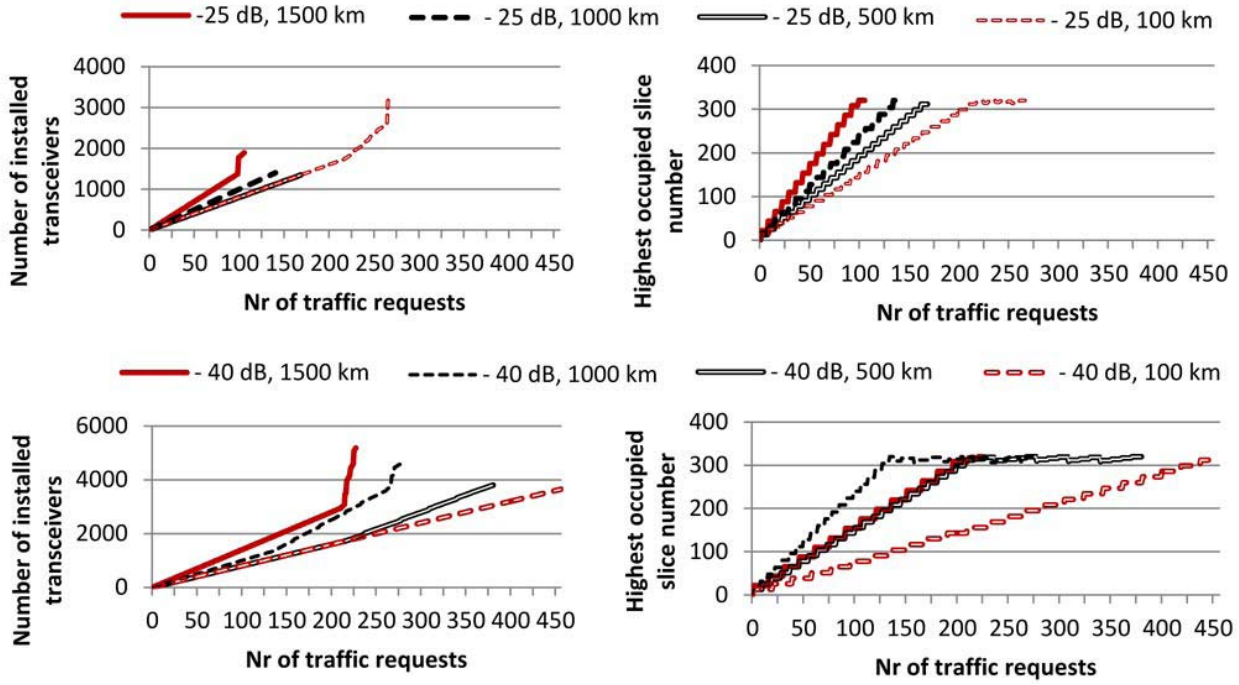

Fig. 4. Number of installed transceivers and right-most occupied slices and versus traffic load when minimizing N_t.

B. Minimization of Spectrum Usage and Transceiver Number

Fig. 4 contains 4 graphs showing the optimal values of N_t (left) and H_s (right) for increasing traffic $|T|$ (curves stop when maximum feasible load is achieved), for both -25 dB (top) and -40 dB (bottom) crosstalk values, and $L = 100, 500, 1000, 1500$ km, obtained when minimizing N_t. Results show that, for low $|T|$, N_t grows linearly until the link spectrum is completely filled (the value of $|T|$ that completely fills the spectrum, let us call it $\hat{T}$, can be easily seen in two graphs on the right of Fig. 4, looking at the values of $|T|$ along the x-axis for which H_s reaches 320 on the y-axis). The optimal solutions for $|T| \leq \hat{T}$ transmit at 28 Gbd[7] and use the most spectrally efficient modulation format with reach higher than L and the cores belonging to a maximal $\gamma_m + 1$-independent subset, where γ_m is highest number of lit neighboring cores tolerated by such modulation format (these solutions could be easily obtained also with Algorithm 2). Then, for $|T| > \hat{T}$, additional cores must be lit (if possible): this imposes the usage of less advanced modulation formats, which in turn causes a sharp increase in N_t. For example, this situation emerges for $L = 100$ km when crosstalk is -25 dB, or for $L = 1500, 1000$ and 500 km in case of -40 dB crosstalk (note the sudden slope increases in the N_t graphs of Fig. 4). In Fig. 6 (left), we plot the percentage of transceivers operating at a given modulation format in the optimal solution minimizing N_t, for increasing traffic load (we fix length to 100 km and a value of -25 dB crosstalk). Results show that, for $|T| \leq \hat{T}$, 28 GBd transceivers using 32-QAM are used, as this choice is the most spectrally efficient. Then, for $|T| > \hat{T}$, the optimal solution adopts 16-QAM, as 16-QAM tolerates a higher number of adjacent lit cores than 32-QAM. Eventually, even 8-QAM is adopted for traffic load above 260 requests (i.e., in correspondence of the second line bending in Fig. 4, top left graph).

Fig. 5 shows N_t (left) and H_s (right) for increasing traffic $|T|$, obtained when minimizing H_s. We observe that the usage of the most efficient modulation format is not always the optimal solution even for low loads. In fact, for some traffic loads, using less advanced modulation formats allows for a more compact spectrum allocation over a larger number of cores, even though each traffic request occupies a larger number of slices. This causes the sawtooth increase of N_t in the right-most graphs of Fig. 5. Also in this case, to get an insight of the modulation-format assignments in the optimal solution, in Fig. 6 (left) we consider a 100 km fiber with -25 dB attenuation and, for each modulation format adopted in the optimal solutions (minimizing H_s), we plot the percentage of transceivers operating at such format versus the traffic load. Results show that 28 GBd transceivers operating at $32, 16$ and 8-QAM coexist (though with variable percentages) in most of the scenarios, whereas 14 GBd transceivers operating at 16-QAM appear only for very low loads.

C. Performance of Heuristic Algorithms for BMSCA

We now evaluate the performance of the heuristic algorithms presented in Section V. In both algorithms, we assume that set K contains the 7 maximal γ-independent sets reported in Fig. 2b)-h), with $0 \leq \gamma \leq 6$.

For the sake of generality, we first report results obtained for traffic requests of variable sizes, obtained by generating random compositions of $|T|$ elements of an overall traffic volume of $|T|$ Tbps, with minimum granularity of 50 Gbps. This way, ranging again $|T|$ from 1 to 460, the total load over the multi-core link and the number of requests are the same as in the sce-

[7]14 Gbd transceivers could be used if their most spectrally efficient modulation format with reach higher than L doubled the spectral efficiency of the most efficient modulation format at 28 Gbd, which never happens when using the reach values reported in Tables I and II.

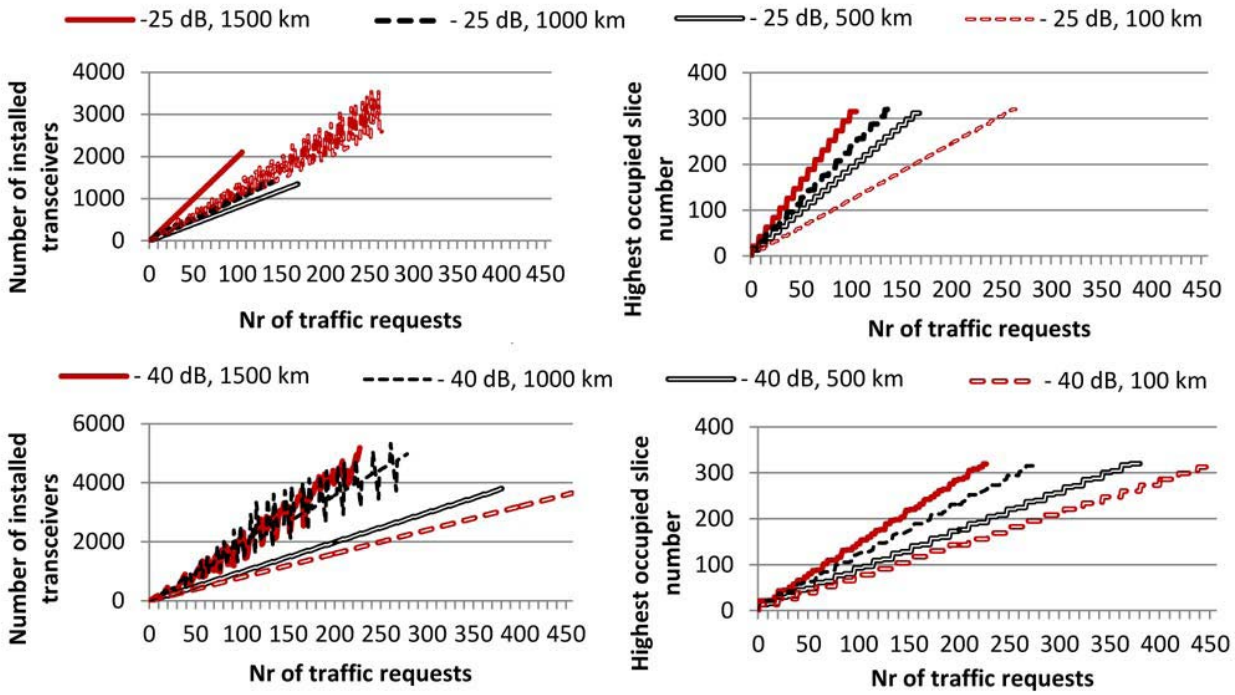

Fig. 5. Number of installed transceivers and right-most occupied slices versus traffic load when minimizing H_s.

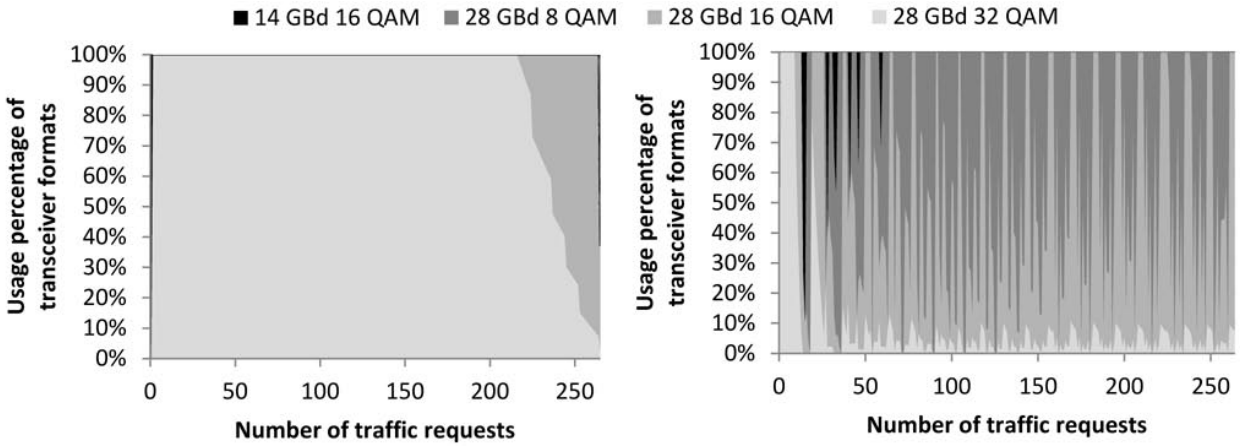

Fig. 6. Modulation formats used when minimizing N_t (left) or H_s (right) for a 100 km fiber with -25 dB attenuation.

nario with fixed 1 Tbps requests. We compare three ordering criteria of the traffic requests based on their volume (see line 10 in Algorithm 1 and line 8 in Algorithm 2): non-decreasing, non-increasing and random order. Due to the lack of space, we only report results obtained for a 1500 km fiber with -40 dB attenuation (results obtained for different fiber lengths and for -25 dB attenuation showed a similar trend). Results are averaged over 50 runs and 95% confidence intervals are reported. As plotted in Fig. 7, the non-increasing ordering criterion provides the best results when minimizing spectrum usage, especially for high link loads. Conversely, results obtained with Algorithm 2 (i.e., when minimizing N_t) did not show significant differences among the three ordering criteria.

In Table III we report some statistics on the percent gap on the values of N_t (left) and H_s (right) obtained with Algorithms 1 and 2 with respect to the optimal values, for both -25 dB and -40 dB crosstalk values. In order to allow for direct comparison with the optimal results presented in the previous subsections, fixed 1 Tbps requests have been considered. Note that the total number of considered scenarios (i.e., the number of instances) varies with the link length and crosstalk values, as we generated one instance for each value of $|T|$ starting from 1 up to the maximum feasible cardinality (i.e. the maximum number of traffic requests that can be feasibly accommodated on the multicore link) which was defined based on the optimal results reported in Figs. 4 and 5. For each combination of crosstalk and fiber-length values, we report the total number of feasible instances obtained via the CPLEX solver, the number of instances for which the heuristic algorithms could not find a feasible solution (though it exists), the number of instances for which the heuristic algorithms could find the optimal solution and the number of instances for which the heuristic solution was below $x\%$ with $x = 5, 10, 15$.

In all the considered scenarios average gaps are below 3%, with the only exception of a 1000 km link with -40 dB

TABLE III
COMPARISON OF RESULTS OBTAINED WITH HEURISTIC ALGORITHMS 1 AND 2 W.R.T. OPTIMAL VALUES, FOR FIBERS WITH −25 dB AND −40 dB ATTENUATION

			Transceiver minimization						Specrtum minimization					
Attenuation per span (dB)	Link length (km)	Inst.	Infeasible inst.	Inst. with 0 % gap	Inst. with gap ≤5 %	Inst. with gap ≤ 10 %	Inst. with gap ≤ 15 %	Average gap (%)	Infeasible inst.	Inst. with 0 % gap	Inst. with gap ≤5 %	Inst. with gap ≤ 10 %	Inst. with gap ≤ 15 %	Average gap (%)
-25	100	269	0	220	262	264	264	0.38	0	111	222	248	259	2.37
-25	500	168	0	168	168	168	168	0	0	168	168	168	168	0
-25	1000	140	0	140	140	140	140	0	0	104	140	140	140	0.19
-25	1500	105	7	98	98	98	98	0	0	105	105	105	105	0
-40	100	456	0	456	456	456	456	0	0	456	456	456	456	0
-40	500	383	0	218	290	354	380	2.62	0	209	362	371	380	1.20
-40	1000	278	0	140	140	149	151	16.97	0	163	258	268	275	1.31
-40	1500	227	0	211	217	217	226	0.61	0	103	170	204	209	2.56

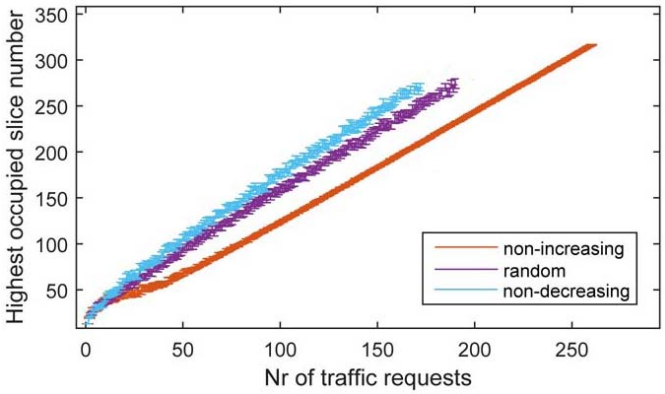

Fig. 7. Average H_s obtained with Algorithm 1 for a 1500 km fiber with -40 dB attenuation, considering random traffic volumes.

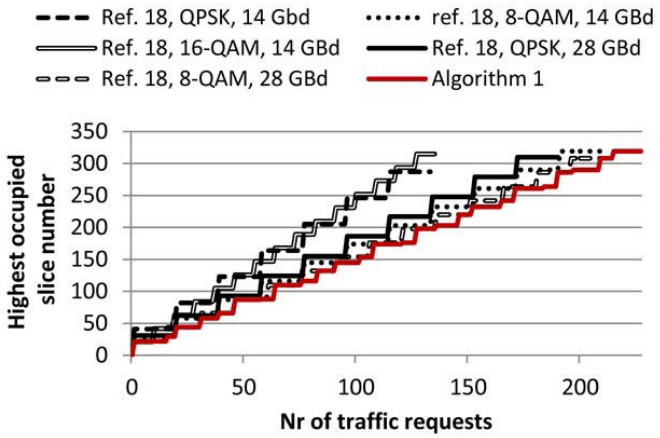

Fig. 8. Performance comparison of Algorithm 1 versus [17, Algorithm 2].

attenuation, for which gaps the average gap is around 17%. As expected, in the case of transceiver minimization, Algorithm 2 always finds optimal values when only the most spectrally-efficient choice of baud rate and modulation formats is used (this happens as long as $|T| < \hat{T}$, i.e. below the x-axis value corresponding to the first change of slope in the left side of the respective graphs in Fig. 4), whereas gaps start to emerge when multiple combinations of baud rates and modulation formats are included in the optimal solution (which happens i.e., for 100 km fibers with −25 dB attenuation and for 500, 1000 and 1500 km fibers with −40 dB attenuation), i.e., when the optimal solution cannot be straightforwardly obtained with a greedy approach.

In more than a half of the considered instances, also Algorithm 1 is able to find optimal solutions when minimizing H_t. Again, this happens when only one choice of baud rate and modulation format is in use (which happens i.e., for 500 and 1500 km fibers with −25 dB attenuation and for 100 km fibers with −40 dB attenuation). In the rest of the instances, gaps rarely exceed 15%. Note that, since in our considered scenarios all the traffic requests have 1 Tbps volume, the impact of the ordering criterion adopted in Algorithms 1 and 2 is eliminated. Note also that the computational times of both algorithms (run over a machine equipped with an Intel i7 processor) were in the order of a few seconds for all the considered scenarios.

Finally, we compare the performance of Algorithm 1 with the RSCA algorithm proposed in [17, Algorithm 2], which aims at minimizing the rightmost occupied slice and works under assumption that a single baud rate and modulation format is used for all the installed transceivers. Therefore, different runs of the algorithm in [17] have been performed, considering every combination of baud rate and modulation format with reach above the link length (at least for the 0 lit neighbor case). For the sake of conciseness, results are reported for a 1500 km fiber with −40 dB attenuation (trends obtained for different fiber lengths and for −25 dB attenuation are similar). As plotted in Fig. 8, Algorithm 1 outperforms the algorithm proposed in [17] for every feasible choice of modulation format and baud rate. This is due to the fact that our proposed algorithm considers solutions where different combinations of baud rates and modulation formats coexist.

VII. CONCLUSIONS

In this paper we investigated the problem of assigning a core, a modulation format and a baud rate to traffic requests over a multicore fiber link. We proved that the problem is NP-hard, we formalized it with two alternative ILPs, and provided effective heuristics to solve it with two different minimization objectives. Our illustrative numerical results confirm that our

heuristic approaches can reach quasi-optimal results in most of the cases, and provide interesting insights on the structure of the optimal solution. For very short links, the optimal solution simply adopts the highest modulation format over all the available cores, but for longer links and high traffic, when crosstalk prevents the utilization of the most spectrally-efficient modulation format, the optimal solution can only be found using more advanced strategies (as the one proposed in this study), that can identify the best trade-off between number and position of lit cores, baud rate and modulation format adopted for transmission over each core in use.

REFERENCES

[1] R.-J. Essiambre, R. Ryf, N. K. Fontaine, and S. Randel, "Breakthroughs in photonics 2012: Space-division multiplexing in multimode and multicore fibers for high-capacity optical communication," *IEEE Photon. J.*, vol. 5, no. 2, Apr. 2013, Art. no. 0701307.

[2] Y. Awaji *et al.*, "High-capacity transmission over multi-core fibers," *Opt. Fiber Technol.*, vol. 35, pp. 100–107, Feb. 2017.

[3] B. Shariati *et al.*, "Impact of spatial and spectral granularity on the performance of SDM networks based on spatial superchannel switching," *J. Lightw. Technol.*, vol. 35, no. 13, pp. 2559–2568, Jul. 1, 2017.

[4] H. Tode and Y. Hirota, "Routing, spectrum and core assignment for space division multiplexing elastic optical networks," in *Proc. 16th Int. Telecommun. Netw. Strategy Planning Symp. (Networks)*, Sep. 2014, pp. 1–7.

[5] D. Klonidis *et al.*, "Spectrally and spatially flexible optical network planning and operations," *IEEE Commun. Mag.*, vol. 53, no. 2, pp. 69–78, Feb. 2015.

[6] T. Mizuno, K. Shibahara, T. Kobayashi, and Y. Miyamoto, "High-capacity dense space division multiplexed multicore fiber transmission," in *Proc. Adv. Photon. (IPR, NOMA, Sensors, Netw., SPPCom, PS)*, 2017, Paper NeTu2B.3.

[7] T. Tanaka *et al.*, "Demonstration of single-mode multicore fiber transport network with crosstalk-aware in-service optical path control," *J. Lightw. Technol.*, vol. 36, no. 7, pp. 1451–1457, Apr. 1, 2018.

[8] M. Gadalla, V. François, and B. Ung, "Spatial light modulator optical switch for multicore fiber," in *Proc. Photon. North (PN)*, Jun. 2018, p. 1.

[9] R. Lin *et al.*, "Real-time 100 gbps/λ/core NRZ and EDB IM/DD transmission over multicore fiber for intra-datacenter communication networks," *Opt. Express*, vol. 26, no. 8, pp. 10519–10526, 2018.

[10] J. Perelló, J. M. Gené, A. Pagès, J. A. Lazaro, and S. Spadaro, "Flex-grid/SDM backbone network design with inter-core XT-limited transmission reach," *IEEE/OSA J. Opt. Commun. Netw.*, vol. 8, no. 8, pp. 540–552, Aug. 2016.

[11] M. Klinkowski, P. Lechowicz, and K. Walkowiak, "Survey of resource allocation schemes and algorithms in spectrally-spatially flexible optical networking," *Opt. Switching Netw.*, vol. 27, pp. 58–78, Jan. 2018.

[12] A. Muhammad, G. Zervas, D. Simeonidou, and R. Forchheimer, "Routing, spectrum and core allocation in flexgrid SDM networks with multi-core fibers," in *Proc. IEEE Int. Conf. Opt. Netw. Design Modeling*, May 2014, pp. 192–197.

[13] A. Muhammad, G. Zervas, G. Saridis, E. H. Salas, D. Simeonidou, and R. Forchheimer, "Flexible and synthetic SDM networks with multi-core-fibers implemented by programmable ROADMs," in *Proc. Eur. Conf. Opt. Commun. (ECOC)*, Sep. 2014, pp. 1–3.

[14] L. Zhang, N. Ansari, and A. Khreishah, "Anycast planning in space division multiplexing elastic optical networks with multi-core fibers," *IEEE Commun. Lett.*, vol. 20, no. 10, pp. 1983–1986, Oct. 2016.

[15] Y. Li, N. Hua, and X. Zheng, "Routing, wavelength and core allocation planning for multi-core fiber networks with MIMO-based crosstalk suppression," in *Proc. Opto-Electron. Commun. Conf. (OECC)*, Jun./Jul. 2015, pp. 1–3.

[16] Y. Li, N. Hua, and X. Zheng, "Capex advantages of multi-core fiber networks," *Photonic Netw. Commun.*, vol. 31, no. 2, pp. 228–238, Apr. 2016.

[17] M. Yang, Y. Zhang, and Q. Wu, "Routing, spectrum, and core assignment in SDM-EONs with MCF: Node-arc ILP/MILP methods and an efficient XT-aware heuristic algorithm," *IEEE/OSA J. Opt. Commun. Netw.*, vol. 10, no. 3, pp. 195–208, Mar. 2018.

[18] J. Perelló, J. M. Gené, J. A. Lazaro, A. Pagès, and S. Spadaro, "Assessment of flex-grid/SDM backbone networks under inter-core XT-limited transmission reach," in *Proc. IEEE Int. Conf. Photon. Switching (PS)*, Sep. 2015, pp. 190–192.

[19] S. Fujii, Y. Hirota, H. Tode, and K. Murakami, "On-demand spectrum and core allocation for reducing crosstalk in multicore fibers in elastic optical networks," *IEEE/OSA J. Opt. Commun. Netw.*, vol. 6, no. 12, pp. 1059–1071, Dec. 2014.

[20] A. Muhammad, G. Zervas, and R. Forchheimer, "Resource allocation for space-division multiplexing: Optical white box versus optical black box networking," *J. Lightw. Technol.*, vol. 33, no. 23, pp. 4928–4941, Dec. 1, 2015.

[21] S. Fujii, Y. Hirota, T. Watanabe, and H. Tode, "Dynamic spectrum and core allocation with spectrum region reducing costs of building modules in AoD nodes," in *Proc. 16th Int. Telecommun. Netw. Strategy Planning Symp. (Networks)*, Sep. 2014, pp. 1–6.

[22] H. Tode and Y. Hirota, "Routing, spectrum, and core and/or mode assignment on space-division multiplexing optical networks," *J. Opt. Commun. Netw.*, vol. 9, no. 1, pp. A99–A113, 2017.

[23] Y. Zhao, R. Tian, X. Yu, J. Zhang, and J. Zhang, "An auxiliary graph based dynamic traffic grooming algorithm in spatial division multiplexing enabled elastic optical networks with multi-core fibers," *Opt. Fiber Technol.*, vol. 34, pp. 52–58, Mar. 2017.

[24] R. Rumipamba-Zambrano, J. Perelló, A. Pagès, J. M. Gené, and S. Spadaro, "Influence of the spatial super channel guard-band width on the performance of dynamic flex-grid/SDM optical core networks," in *Proc. 18th Int. Conf. Transparent Opt. Netw. (ICTON)*, 2016, pp. 1–4.

[25] R. Luo, N. Hua, Y. Li, X. Zheng, and B. Zhou, "Fast parallel lightpath re-optimization for crosstalk reduction in multi-core fiber networks," in *Proc. Opt. Fiber Commun. Conf. Expo. (OFC)*, 2017, pp. 1–3.

[26] Y. Tan *et al.*, "Distance adaptive routing, core and spectrum allocation in space division multiplexing optical networks with multi-core fibers," in *Proc. Asia Commun. Photon. Conf.*, 2016, Paper AF2A–159.

[27] Y. Tan *et al.*, "Crosstalk-aware provisioning strategy with dedicated path protection for elastic multi-core fiber networks," in *Proc. 15th Int. Conf. Opt. Commun. Netw. (ICOCN)*, Sep. 2016, pp. 1–3.

[28] C. Rottondi, P. Martelli, P. Boffi, L. Barletta, and M. Tornatore, "Modulation format, spectrum and core assignment in a multicore flexi-grid optical link," in *Proc. Opt. Fiber Commun. Conf. Expo. (OFC)*, Mar. 2018, pp. 1–3.

[29] J. Sakaguchi *et al.*, "305 Tb/s space division multiplexed transmission using homogeneous 19-core fiber," *J. Lightw. Technol.*, vol. 31, no. 4, pp. 554–562, Feb. 15, 2013.

[30] S. LaRochelle, C. Jin, and Y. Messaddeq, "Design and characterization of multicore erbium-doped fibers," in *Proc. 42nd Eur. Conf. Opt. Commun. (ECOC)*, Sep. 2016, pp. 1–3.

[31] J. Sakaguchi *et al.*, "19-core MCF transmission system using EDFA with shared core pumping coupled via free-space optics," *Opt. Express*, vol. 22, no. 1, pp. 90–95, 2014.

[32] P. Poggiolini, "The GN model of non-linear propagation in uncompensated coherent optical systems," *IEEE/OSA J. Lightw. Technol.*, vol. 30, no. 24, pp. 3857–3879, Dec. 15, 2012.

[33] P. Martelli, "Impact of the crosstalk in space-division multiplexing," in *Proc. IEEE 19th Int. Conf. Transparent Opt. Netw. (ICTON)*, Jul. 2017, pp. 1–4.

[34] S. Ö. Arık, K.-P. Ho, and J. M. Kahn, "Optical network scaling: Roles of spectral and spatial aggregation," *Opt. Express*, vol. 22, no. 24, pp. 29868–29887, 2014.

[35] M. Blidia, M. Chellali, O. Favaron, and N. Meddah, "Maximal k-independent sets in graphs," *Discussiones Mathematicae Graph Theory*, vol. 28, no. 1, pp. 151–163, 2008.

[36] M. R. Garey and D. S. Johnson, *Computers and Intractability: A Guide to the Theory of NP-Completeness*. New York, NY, USA: Freeman, 1979.

[37] M. Pfund, J. W. Fowler, and J. N. D. Gupta, "A survey of algorithms for single and multi-objective unrelated parallel-machine deterministic scheduling problems," *J. Chin. Inst. Ind. Eng.*, vol. 21, no. 3, pp. 230–241, 2004.

[38] L. Fanjul-Peyro and R. Ruiz, "Iterated greedy local search methods for unrelated parallel machine scheduling," *Eur. J. Oper. Res.*, vol. 207, no. 1, pp. 55–69, 2010.

[39] O. H. Ibarra and C. E. Kim, "Heuristic algorithms for scheduling independent tasks on nonidentical processors," *J. ACM*, vol. 24, no. 2, pp. 280–289, Apr. 1977.

Authors' photographs and biographies not available at the time of publication.